

3<sup>rd</sup> REVISED VERSION

## Trimethylangelicin Reduces IL-8 Transcription and Potentiates CFTR Function

Anna Tamanini,<sup>1\*</sup> Monica Borgatti,<sup>2\*</sup> Alessia Finotti,<sup>2\*</sup> Laura Piccagli,<sup>2</sup> Valentino  
Bezzerri,<sup>1</sup> Maria Favia,<sup>3</sup> Lorenzo Guerra,<sup>3</sup> Ilaria Lampronti,<sup>2</sup> Nicoletta Bianchi,<sup>2</sup>  
Francesco Dall'Acqua,<sup>4</sup> Daniela Vedaldi,<sup>4</sup> Alessia Salvador,<sup>4</sup> Enrica Fabbri,<sup>2</sup> Irene  
Mancini,<sup>2</sup> Elena Nicolis,<sup>1</sup> Valeria Casavola,<sup>3\*\*</sup> Giulio Cabrini<sup>1\*\*</sup>  
and Roberto Gambari<sup>2,5\*\*</sup>

<sup>1</sup>Laboratory of Molecular Pathology, Laboratory of Clinical Chemistry and Haematology, University-Hospital, Verona, Italy

<sup>2</sup>BioPharmaNet, ER-GenTech, Department of Biochemistry and Molecular Biology, University of Ferrara, Italy

<sup>3</sup>Department of General and Environmental Physiology, University of Bari, Italy

<sup>4</sup>Department of Pharmaceutical Sciences, University of Padova, Italy

<sup>5</sup>Department of Biochemistry and Molecular Biology, University of Ferrara, Italy

Correspondence should be addressed to: Dr. Giulio Cabrini, Laboratory of Molecular Pathology, University Hospital of Verona, Verona, Italy (Phone +39-045-8122457; fax +39-045-8122840; e-mail: [giulio.cabrini@univr.it](mailto:giulio.cabrini@univr.it)) or Prof. Roberto Gambari, Department of Biochemistry and Molecular Biology, University of Ferrara, Via Fossato di Mortara 74, 44100 Ferrara, Italy (Phone: +39-532-424443; fax: +39-532-424500; e-mail: [gam@unife.it](mailto:gam@unife.it))

Running title: Trimethylangelicin and lung inflammation

\* AT, MB and AF contributed equally to this work

\*\* RG, GC and VC share senior authorship

This work was supported by grants from the Italian Cystic Fibrosis Research Foundation (grant FFC #13/2007, FFC #18/2009 and FFC #17/2010) with the contribution of "Associazione Veneta per la lotta alla fibrosi cistica", "Delegazione FFC Belluno", "Delegazione FFC Torino" (to GC and RG), the Fondazione Cariparo (to RG) and MUR COFIN-2007 (to RG). We wish to thank "Centro di Eccellenza di Genomica in campo biomedico e agrario", CEGBA. VB is fellow of the Italian Cystic Fibrosis research Foundation (FFC), EN is fellow of the "Azienda Ospedaliera Universitaria Integrata di Verona".

## Abstract

Chronic inflammatory response in the airway tract of patients affected by cystic fibrosis is characterized by an excessive recruitment of neutrophils to the bronchial lumina, driven by the chemokine Interleukin (IL)-8. We previously found that 5-methoxypsoralen reduces *P.aeruginosa*-dependent IL-8 transcription in bronchial epithelial cell lines, with an IC<sub>50</sub> of 10 μM. Here, we extended the investigation to analogues of 5-methoxypsoralen and we found that the most potent effect is obtained with 4,6,4'-trimethylangelicin (TMA), which inhibits *P.aeruginosa*-dependent IL-8 transcription at nanomolar concentration in IB3-1, CuFi-1, CFBE410<sup>o</sup> and Calu-3 bronchial epithelial cell lines. Analysis of phosphoproteins involved in proinflammatory transmembrane signaling evidenced that TMA reduces the phosphorylation of RSK1 and AKT2/3, which we found indeed involved in *P.aeruginosa*-dependent activation of IL-8 gene transcription by testing the effect of pharmacological inhibitors. In addition, we found a docking site of TMA into NF-kB by *in silico* analysis, whereas inhibition of the NF-kB/DNA interactions *in vitro* by EMSA was observed at high concentrations (10 mM TMA). In order to further understand whether NF-kB pathway should be considered a target of TMA, Chromatin Immunoprecipitation was performed, and we observed that TMA (100 nM) pre-incubated in whole living cells reduced the interaction of NF-kB with the promoter of IL-8 gene. These results suggest that TMA could inhibit IL-8 gene transcription mainly by intervening on driving the recruitment of activated transcription factors on IL-8 gene promoter, as demonstrated here for NF-kB. Although the complete understanding of the mechanism of action of TMA deserves further investigation, an activity of

TMA on phosphorylating pathways was already demonstrated by our study. Finally, since psoralens have been shown to potentiate CFTR-mediated chloride transport, TMA was tested and found to potentiate CFTR-dependent chloride efflux. In conclusion, TMA is a dual-acting compound reducing excessive IL-8 expression and potentiating CFTR function.

Keywords: psoralens; angelicin; trimethylangelicin; lung inflammation; cystic fibrosis.

Abbreviations: CF, cystic fibrosis; IL, interleukin; ANG, angelicin; PSR, psoralen; TMA, 4,6,4'-trimethylangelicin; TMP, 4,5',8-trimethylpsoralen; qRT-PCR, quantitative reverse transcription polymerase-chain reaction.

## INTRODUCTION

Cystic fibrosis (CF) is a severe genetic disease due to defects of the Cystic Fibrosis Transmembrane conductance Regulator (CFTR) gene (for review see 39). CF affects several organs with the chronic pulmonary disease being the major cause of reduction of the quality and expectancy of life. Hallmark of CF lung disease is chronic infection sustained by the gram negative bacterium *Pseudomonas aeruginosa* and excessive lung inflammation with a huge infiltrate of neutrophils in the bronchial lumen, mainly due to the release of the chemokine interleukin (IL)-8 (2, 4, 5, 11, 24, 27, 36). The identification of novel drugs, to reduce the excessive lung inflammation in CF, is considered a key therapeutic target to circumvent progressive lung tissue deterioration (for review see 25).

Psoralens are well known furocoumarins belonging to the class of photosensitizers used for their activity in the treatment of various chronic inflammatory skin diseases (6, 7, 12, 13, 23, 30, 37), and they are characterized by a differently substituted tricyclic aromatic skeleton, derived from condensation of a coumarin nucleus with a furan ring. Among psoralens-related compounds, the angular angelicin-like isomers are both synthetic and natural compounds, e.g. derived from the medicinal plant *Angelica arcangelica*, that could exhibit interesting pharmacological activity when compared with linear psoralens, showing low toxicity and low DNA-binding activity (6, 23).

As far as lung inflammation in CF is concerned, we have preliminary indications that 10  $\mu$ M 5-methoxypsoralen inhibits IL-8 transcription in bronchial epithelial cells exposed to *P.aeruginosa*, thus suggesting the potential usefulness of psoralens in the regulation of pro-inflammatory genes and strengthening the idea of searching for more potent analogues for this application (33). The aim of the

present study is to determine the activity of the four psoralens on the expression of IL-8 gene, the major chemokine released from CF cells infected by *Pseudomonas aeruginosa* (19). The psoralens studied here, and described in Fig. 1, have been chosen as prototypes of linear versus angular and of non-methylated versus trimethylated structures, namely psoralen (PSR), angelicin (ANG), 4,5',8-trimethylpsoralen (TMP), 4,6,4'-trimethylangelicin (TMA). Since psoralen-like structure might lead to alteration of the NF- $\kappa$ B signaling (35), the potential effect of TMA on the modulation of the interaction of the Nuclear Factor(NF)- $\kappa$ B with target DNA sequences was investigated by *in silico* docking analysis, Electrophoretic Mobility Shift Assay (EMSA) and Chromatin immunoprecipitation (ChIP) of IL-8 promoter. Moreover, since psoralens have been shown to be potentiators of CFTR function (17), we have investigated the effect of the most effective psoralen analogue here described on the activation of CFTR-mediated chloride efflux. The present results here identify TMA as a compound acting both as a strong inhibitor of *P.aeruginosa*-dependent expression of IL-8 and as a potentiator of CFTR-mediated chloride efflux.

## **MATERIALS AND METHODS**

### **Compounds**

Angelicin [2-Oxo-(2H)-furo-[2,3-h]-1-benzopyran], was purchased from Sigma/Aldrich (Milwaukee, WI, USA). Psoralen, 4,5',8-trimethylpsoralen and 4,6,4'-trimethylangelicin were synthesized at the Dept. of Pharmaceutical Sciences, University of Padova, Italy (Figure 1).

### **Cell Cultures**

IB3-1 cells, derived from a CF patient with a F508del/W1282X mutant genotype were grown as previously described (3, 8, 15, 16, 32); non CF Calu-3, a cell line obtained from a human lung adenocarcinoma derived from submucosal gland of proximal bronchial airways, and CF CuFi-1 cell line, obtained from human bronchial epithelium derived from a CF patient with a F508del/F508del mutant genotype, were cultured on transwell membranes (41). The cells were seeded at density of 600,000 cells/cm<sup>2</sup> onto collagen coated Transwell polyester membranes (0.33 cm<sup>2</sup>, 0.4 μm pore size) (Becton Dickinson, Franklin Lakes, NJ). The experiments were performed when the cell monolayers reached a TER > 1500 Ω x cm<sup>2</sup>. CFBE41o- cells homozygous for the F508del allele (F508del/F508del), were a generous gift of Professor D. Gruenert, University of California at San Francisco, and CFBE41o-/sNHERF1 were CFBE41o- cells stably transfected with cDNA encoding wt NHERF1 (20). For chloride efflux experiments the cells were seeded on 0.4-μm pore size PET filter inserts (Falcon Becton-Dickinson Labware, USA).

## **Cell Infection, quantification of transcripts of inflammatory genes and IL-8 protein**

Cells were starved and treated with different psoralens for 20 hours before infection, which was performed as previously described (3, 8, 15, 16, 32). Quantification of transcripts of inflammatory genes was performed by qRT-PCR, proliferation and antibacterial assays were done as previously described (32, 33). IL-8 secretion was assessed at different doses of TMA added for 20 hours, then media and TMA were freshly added and collected after four hours of PAO1 infection. IL-8 was measured by ELISA (Bender MedSystems, Wien, Austria), in duplicate according to the manufacturer's instructions

## **Fluorescence measurements of apical chloride efflux**

Chloride efflux was measured using the  $\text{Cl}^-$  sensitive dye MQAE (20). Confluent Calu-3 cell monolayers were loaded overnight in culture medium containing 5 mM MQAE at 37°C in a  $\text{CO}_2$  incubator and then inserted into a perfusion chamber that allowed independent perfusion of apical and basolateral cell surfaces. The apical  $\text{Cl}^-$  efflux measurements were performed when the confluent cell monolayers reached a transepithelial resistance  $>1500 \Omega \times \text{cm}^2$  for Calu-3 and  $>300 \Omega \times \text{cm}^2$  for CFBE410- and CFBE410-/sNHERF1. Fluorescence was recorded with a Cary Eclipse Varian spectrofluorometer. To measure chloride efflux rate across the apical membrane, the apical perfusion medium was changed with a medium in which chloride was substituted with iso-osmotic nitrate. All experiments were performed at 37°C in HEPES-buffered bicarbonate-free media ( $\text{Cl}^-$  medium, in

millimolar: NaCl 135, KCl 3, CaCl<sub>2</sub> 1.8, MgSO<sub>4</sub> 0.8, HEPES 20, KH<sub>2</sub>PO<sub>4</sub> 1, glucose 11, and Cl<sup>-</sup> free-medium: NaNO<sub>3</sub> 135, KNO<sub>3</sub> 3, MgSO<sub>4</sub> 0.8, KH<sub>2</sub>PO<sub>4</sub> 1, HEPES 20, Ca(NO<sub>3</sub>)<sub>2</sub> 5, glucose 11). We measured the apical CFTR-dependent chloride secretion as previously described (20): CFTR-dependent chloride secretion was calculated as the difference in the rate of change of forskolin (FSK) stimulated fluorescence in the absence or presence of apical treatment with the specific CFTR inhibitor, CFTR<sub>inh</sub>-172 (28).

### **Phosphokinase Array**

The phosphorylation pattern of kinases was determined with the Human Phospho-MAPK Array Kit (R&D Systems, Inc., Minneapolis, MN, USA) according to the manufacturer's instructions. Briefly, CuFi-1 cells were seeded into four Petri dishes (2.5 x 10<sup>6</sup> in 6-cm diameter) to obtain 1 x 10<sup>7</sup> cells for each array. Serum free medium was replaced and 100 nM TMA or solvent alone was added to the cells for 20 hours before the infection for an additional 30 minutes. Cell lysates (200 µg) were incubated with each array. After incubation of the arrays with anti-phospho-MAPK antibody cocktail, streptavidin – HRP and washes, the membranes were exposed to chemiluminiscent reagent and subjected to X-ray films. The signal of the spots developed on X-ray films were quantified by scanning the film on a high resolution transmission-mode scanner and analyzing the array image file using the image analyses software Digimizer (MedCalc Software, Mariakerke, Belgium).



### **Signal transduction inhibitors**

Triciribine hydrate ( $C_{13}H_{16}N_6O_4 \cdot xH_2O$ ) was obtained from Sigma/Aldrich (Milwaukee, WI, USA) and SL 0101-1 (3-[(3,4-Di-O-acetyl-6-deoxy- $\alpha$ -L-mannopyranosyl)oxy]-5,7-dihydro-2-(4-hydroxyphenyl)-4H-1benzopyran-4-one) from Tocris Bioscience (Missouri, USA). Stock solution of Triciribine hydrate (10 mM) in dimethyl sulfoxide (DMSO) and SL 0101-1 (20 mM) in ethanol were stored at  $-20^{\circ}C$ . The inhibitors were diluted into medium before addition to cells.

### **Docking of TMA into the DNA binding motif of NF- $\kappa$ B.**

TMA was docked into putative binding site of the NF- $\kappa$ B targets employing Glide software (27 of JMC) as described elsewhere (29, 35). TMA were docked again into DNA recognition site, using the CPU time-intensive and accurate Extra-Precision (XP) method.

### **Electrophoretic Mobility Shift Assay (EMSA).**

EMSA was performed as previously described (8-10) Briefly, double-stranded synthetic oligodeoxynucleotides mimicking the NF- $\kappa$ B binding (NF- $\kappa$ B, sense: 5'-CGC TGG GGA CTT TCC ACG G-3') have been employed. Oligodeoxynucleotides were labeled with  $\gamma^{32}$ -P-ATP using 10 Units of T4-poly-nucleotide-kinase (MBI Fermentas) in 500 mM Tris-HCl, pH 7.6, 100 mM  $MgCl_2$ , 50 mM DTT, 1 mM spermidine, 1 mM EDTA in the presence of 50 mCi  $\gamma^{32}$ P-ATP) in a volume of 20  $\mu$ l for 45 minutes at  $37^{\circ}C$ . Reaction was brought to 150 mM NaCl and 150 ng complementary oligodeoxynucleotide was added. Reaction temperature was increased to  $100^{\circ}C$  for 5 minutes and left

diminishing to room temperature overnight. Binding reactions were set up as described elsewhere (9) in a total volume of 20  $\mu$ l containing buffer TF plus 5% glycerol, 1 mM dithiothreitol, 10 ng of human NF- $\kappa$ B p50 protein with or without 10 ng of NF- $\kappa$ B p65 protein (Promega) and different concentrations of compounds. After an incubation of 20 min at room temperature, 0.25 ng of  $^{32}$ P-labeled oligonucleotides were added to the samples for further 20 min at room temperature and then they were electrophoresed at constant voltage (200 V) under low ionic strength conditions (0.25x TBE buffer: 22 mM Tris borate, 0.4 mM EDTA) on 6% polyacrylamide gels. Gels were dried and subjected to standard autoradiographic procedures (10).

#### **Chromatin Immunoprecipitation (ChIP) assay**

Chromatin immunoprecipitation assays were performed by using the Chromatin Immunoprecipitation Assay Kit (Upstate Biotechnology Inc., Lake Placid, NY, USA) as previously described (21, 22). Briefly, a total of  $5 \times 10^6$  IB3 cells (from two 6-cm diameter Petri dishes) were treated, for 10 min at room temperature, with 1% formaldehyde culture medium. Cells were washed in phosphate-buffered saline, and then glycine was added to a final concentration of 0.125 M. The cells were then suspended in 0.5 ml of lysis buffer (1% SDS, 10 mM EDTA, and 50 mM Tris-Cl, pH 8.1) plus protease inhibitors (1  $\mu$ g/ml pepstatin A, 1  $\mu$ g/ml leupeptin, 1  $\mu$ g/ml aprotinin, and 1 mM phenylmethylsulfonyl fluoride) and the chromatin subjected to sonication (using a Sonics Vibracell VC130 sonicator with a 2-mm probe). Fifteen 15-s sonication pulses at 30% amplitude were required to shear chromatin to 200-1000 bp fragments. 0.2-ml aliquots of chromatin were diluted to 2 ml in ChIP

dilution buffer containing protease inhibitors and then cleared with 75  $\mu$ l of salmon sperm DNA/protein A-agarose 50% gel slurry (Upstate Biotechnology) for 1 h at 4°C before incubation on a rocking platform with either 10  $\mu$ g of NF- $\kappa$ B p65 specific antiserum (sc-372X, Santa Cruz Biotechnology Inc., Santa Cruz, CA, USA) or normal rabbit serum (Upstate Biotechnology). 20  $\mu$ l of diluted chromatin was saved and stored for later PCR analysis as 1% of the input extract. Incubations occurred overnight at 4 °C and continued an additional 1 h after the addition of 60  $\mu$ l protein A-agarose slurry. Thereafter the agarose pellets were washed consecutively with low salt, high salt and LiCl buffers. DNA/protein complexes were recovered from the pellets with elution buffer (0.1 M NaHCO<sub>3</sub> with 1% SDS), and cross-links were reversed by incubating overnight at 65 °C with 0.2 M NaCl. The samples were treated with RNase A and proteinase K, extracted with phenol/chloroform and ethanol-precipitated. The pelleted DNAs were washed with 70% ethanol and dissolved in 40  $\mu$ l of Tris/EDTA. 2  $\mu$ l aliquots were used for each real-time PCR reaction to quantitate immunoprecipitated promoter fragments.

### **Real-time PCR Quantitation of Immunoprecipitated Promoter Fragments**

For quantitative real-time PCR reaction, a pair of primers that amplify a 301 bp region on the IL-8 promoter, containing the NF- $\kappa$ B binding site, was designed (forward: 5'-TCA CCA AAT TGT GGA GCT TCA GTA T-3', reverse: 5'-GGC TCT TGT CCT AGA AGC TTG TGT-3'). PCR reactions were also performed using negative control primers that amplify a 255 bp genomic region about 5 kb upstream of the IL-8 promoter, lacking NF- $\kappa$ B binding sites (forward: 5'-TCC CTA AGT CAC TTT CTT CAA GTT GC-3', reverse: 5'-CGT GCA TTT

AAT TGT GTC TTG TGG-3'). Each Real-time PCR reactions were performed in 25  $\mu$ l of final volume, using 2  $\mu$ l of template DNA (from chromatin immunoprecipitations), 10 pmol of primers and 1 x iQ™ SYBR® Green Supermix (Bio-Rad) for a total of 45 cycles (96°C for 15 s, 66°C for 30 s, and 72°C for 20 s) using an iCycler IQ® (Bio-Rad). The relative proportions of immunoprecipitated promoter fragments were determined based on the threshold cycle ( $T_c$ ) value for each PCR reaction. Real time PCR data analysis were obtained using the comparative cycle threshold method: a  $\Delta T_c$  value was calculated for each sample by subtracting the  $T_c$  value for the sample amplify with IL-8 promoter primers from the  $T_c$  value obtained for the same sample amplify with negative control primers. For each kind of immunoprecipitation (Igg or NF-kB p65 antiserum), a  $\Delta\Delta T_c$  value was then calculated by subtracting the  $\Delta T_c$  value for the untreated cells sample from the  $\Delta T_c$  value for the treated cells samples. Fold differences were then determined by raising -2 to the  $\Delta\Delta T_c$  power. Each sample was quantitated in duplicate on at least three separate experiments. Mean  $\pm$  S.D. values were determined.

### **Statistics**

Results are expressed as mean  $\pm$  standard error of the mean (SEM). Comparisons between groups were made by Student's  $t$  test for paired or unpaired data. Statistical significance was defined with  $p < 0.05$  (\*),  $p < 0.01$  (\*\*) and  $p < 0.001$  (\*\*\*)

## RESULTS

### **Linear and angular psoralens inhibit IL-8 mRNA transcription in cells infected with *P.aeruginosa*.**

To determine the activity of the four psoralen derivatives of this study (psoralen (PSR), 4,5',8-trimethylpsoralen (TMP), angelicin (ANG) and 4,6,4'-trimethylangelicin (TMA), we utilized CF (IB3-1, CuFi-1, CFBE41o-) and non-CF bronchial epithelial cell lines (Calu-3). None of the psoralen derivatives had any effect on cell proliferation or bacterial growth (see Supplementary material, Figure S1 and S2). Figure 2 shows their effects on IL-8 transcription in the cystic fibrosis cells, IB3-1, that had been preincubated with psoralens for 20 hours, then infected with *P. aeruginosa* (PAO1 laboratory strain) for a further 4 hours. PSR reduced IL-8 mRNA accumulation by an average 50% starting from 0.1  $\mu\text{M}$  concentration and reached 80% inhibition at 100  $\mu\text{M}$  (Figure 2A), TMP by an average of 40% inhibition starting from 0.01  $\mu\text{M}$  (Figure 2B), ANG by an average of 50% inhibition starting from 5  $\mu\text{M}$  and TMA by an average of 70% inhibition starting from 1 nM. This first set of experiments suggests that methylation, which leads to an enhancement of lypophilicity, is a key feature to increase the inhibitory activity of both linear and angular psoralens, being the trimethylated angular compound TMA the most potent derivative. To verify whether the inhibition of *P.aeruginosa*-dependent transcription of IL-8 mRNA observed in IB3-1 cells is reproducible in other bronchial epithelial cells and whether it is specific for CF-cells, linear psoralens were next tested in the non-CF cell line Calu-3, grown polarized on Transwell filters. Cells were treated on both the apical and basolateral sides with the linear psoralens PSR or TMP (10  $\mu\text{M}$  for 20 hours) and

the cells were then exposed to PAO-1 ( $2 \times 10^7$  CFU/ml) on the apical side for a further 4 hours. Analysis of bacterial-evoked pro-inflammatory signaling was extended to other key genes involved in the chemotaxis of leukocytes besides IL-8, namely the adhesion molecule ICAM-1 and the chemokines GRO $\alpha$ , GRO $\gamma$ , MIP-1 $\alpha$  and IP-10. As shown in Fig. 3, the inhibitory effect of PSR and TMP was reproducible also in polarized, non-CF Calu-3 cells and was mainly restricted to IL-8 transcription.

Angular psoralens were tested in both the non-CF Calu-3 and CF CuFi-1 cell lines and, in both cases, Angelicin (10  $\mu$ M) inhibited mainly the *P.aeruginosa*-dependent transcription of IL-8 mRNA, as shown in Figure 4. Since the trimethylated angular psoralen TMA was the most potent compound inhibiting IL-8 transcription in IB3-1 cells, a dose-response experiment of TMA was performed in CuFi-1 cells. As shown in Fig 5, preincubation of TMA in CuFi-1 cells strongly inhibited IL-8 mRNA expression and release of IL-8 protein starting from nanomolar concentrations. Conversely, simultaneous addition of 100 nM TMA with *P.aeruginosa* did not produce a significant inhibition. To test the effect of TMA in polarized bronchial epithelial cells, 100 nM TMA was preincubated in different CF and non-CF cells. The inhibitory effect of TMA was reproducible also in polarized cells grown on Transwell inserts, as Calu-3, CuFi-1, CFBE41o- and CFBE41o-/sNHERF1 cell monolayers, where the mutated F508del CFTR has been rescued to the apical cell surface by NHERF1 stable overexpression (20), as shown in Figs. 6 and 7.

All these results considered, trimethylation and angular structure confer the highest inhibitory potency to these psoralen analogues. In particular, TMA is a strong inhibitor of *P.aeruginosa*-dependent IL-8 transcription, starting from

nanomolar concentrations in at least four different CF and non-CF bronchial epithelial cell lines.

### **Effect of TMA on CFTR-mediated chloride efflux in bronchial epithelial cells**

Since psoralens such as 5- and 8-methoxypsoralen, PSR, TMP and angelicin have been previously shown to potentiate CFTR-mediated chloride transport (17), the effect of TMA on CFTR-mediated chloride efflux was tested in Calu-3 polarized cell monolayers. Figure 8 illustrates typical experiments and the summaries of different experiments of chloride efflux performed in Calu-3 polarized cell monolayers treated (C and D) or not (A and B) with 250 nM TMA. As shown in Figure 8 D, a 15 min preincubation with TMA strongly increased the CFTR-dependent chloride efflux. Dose-response experiments were then performed to determine the minimum concentration of TMA that potentiates chloride efflux. As reported in Fig. 9 A, TMA significantly increased the average FSK stimulation of CFTR-dependent chloride efflux starting from 100 nM concentration. Moreover, in order to test whether TMA can also potentiate the transport activity of F508delCFTR that has been rescued to the apical membrane, we determined the effect of TMA on the chloride efflux in CFBE41o-/sNHERF1 cell monolayers where the mutated F508del CFTR has been rescued to the apical cell surface by NHERF1 stable overexpression (20). As shown in Fig. 9 B, TMA (250 nM) significantly doubled F508del CFTR-dependent chloride efflux rescued in CFBE41o-/sNHERF1 while it was ineffective in CFBE41o- cells. Altogether, these results indicate that TMA treatment is able to potentiate the apical

chloride efflux mediated both by wild-type and by mutated CFTR rescued on the apical membrane of polarized bronchial epithelial cell monolayers.

#### **Effect of TMA on phosphoprotein phosphorylation in CuFi-1 cells.**

To investigate the potential effect of TMA on phosphoproteins involved in the proinflammatory signaling leading to IL-8 transcription, extracts of CuFi-1 cells preincubated with TMA and exposed to *P.aeruginosa* were analyzed with a Human Phospho-MAPK Array assay. Figure 10 indicates that *P.aeruginosa* induces the phosphorylation of several known protein substrates, such as the MAP Kinases p38, ERK1/2, JNK 1/2/3 and, newly reported here, of RSK1/2, MSK2, HSP27, GSK-3 and AKT1/2/3. As far as the effect of TMA is concerned, the results presented in Fig. 10 panel A and B indicate that preincubation of TMA further increases the phosphorylation on MAPK ERK and JNK, whereas it reduces that of RSK1 and AKT 2/3. To obtain preliminary insights on whether the inhibitory effect of TMA on IL-8 expression and release could be mediated by the reduced phosphorylation of RSK1 and AKT, we tested the effect of known pharmacological inhibitors of these kinases on *P.aeruginosa*-dependent transcription of IL-8 gene. As shown in Fig. 10 C, both triciribine hydrate, which is known to inhibit Akt 1/2/3, and SL 0101-1, which is known to inhibit RSK, reduced IL-8 mRNA accumulation by an average of 35-45%, suggesting that RSK1 and AKT could be involved in the reduction of IL-8 gene expression mediated by TMA.



### **Effect of TMA on the interaction of NF-kB with IL-8 gene promoter.**

Transcription of IL-8 gene in human bronchial epithelial cells exposed to *P.aeruginosa* is known to be regulated by the interaction of the nuclear transcription factor NF-kB with the IL-8 gene promoter, as evidenced by previous mechanistic studies and confirmed by interfering experiments utilizing transcription factor decoy oligodeoxynucleotides (3). Therefore, we reasoned whether the inhibitory effect of TMA could be at least in part related to a reduction in the NF-kB dependent regulation of the IL-8 gene transcription. To explore this possibility, we performed experiments based on three complementary approaches: (a) *in silico* docking analysis, (b) Electrophoretic Mobility Shift Assay (EMSA) and (c) Chromatin immunoprecipitation (ChIP). The results of the first two approaches are depicted in Figure 11, which clearly indicates that TMA is able to bind to NF-kB (*in silico* docking analysis, panel A) and inhibits the NF-kB/DNA interactions (EMSA studies, panels B-D). The inhibitory effects on NF-kB/DNA interactions were reproducibly obtained using NF-kB p50 (Figure 11B), reconstituted p50/p65 heterodimer (Figure 11C) and unfractionated nuclear factors from IB3-1 cells (Figure 11D). No major differences were found when TMA was first added to the target NF-kB oligonucleotide (Figure 11B, upper panel) or to NF-kB p50 (Figure 11B, lower panel). In addition, ChIP analysis demonstrates that TMA strongly reduces to recruitment of NF-kB to the IL-8 gene promoter. IB3-1 cells were treated with PAO-1 or PAO-1 plus TMA, nuclear/DNA interactions stabilized by formaldehyde treatment and the shared chromatin immunoprecipitated with antibodies against NF-kB. In parallel, the same procedure was performed with control untreated IB3-1

cells. The DNA from immunoprecipitates was isolated and PCR-amplified with primers specific for the IL-8 promoter (Figure 12A). Quantitative real-time PCR profiles for the amplification of the IL-8 promoter are shown in Figure 12C and 12D and demonstrate that treatment of IB3-1 cells with PAO-1 induces a fast and sharp recruitment of NF- $\kappa$ B to the IL-8 gene promoter. This effect is inhibited by in the presence of TMA.

## DISCUSSION

The most important finding of this paper is that the trimethylated angular psoralen TMA is a strong inhibitor of the expression of the IL-8 gene in bronchial epithelial cells in which the inflammatory response has been challenged with *P.aeruginosa*, the most common bacterium found in the airways of patients affected by CF. This effect (a) was obtained at low (nanomolar) concentrations of the molecule; (b) is not accompanied by a reduction of cell growth; (c) was independent of the expression of wild type or mutated CFTR and (d) appeared to be relatively specific for IL-8, as little or no inhibitory effect was observed on the accumulation of other pro-inflammatory transcripts, such as those encoded by ICAM-1, GRO $\alpha$ , GRO $\gamma$ , MIP-1 $\alpha$  and IP-10. Moreover, TMA strongly potentiates chloride efflux through both wild-type and mutated CFTR that has been rescued on the apical membrane. Altogether, these results indicate that TMA is a promising dual-acting compound to be investigated both as a modulator of the critical step of the excessive IL-8-mediated inflammatory response and as potentiator of the function of chloride transport through mutated CFTR protein.

The effect of TMA on IL-8 gene transcription is of great interest considering that IL-8 is the most abundant chemokine found in the bronchoalveolar fluid of CF patients (5). As a matter of fact, IL-8 drives the recruitment of the excessive amount of neutrophils found in CF bronchial lumens, which untowardly contributes to the progressive lung tissue damage and respiratory insufficiency of these patients, mainly upon release of different kinds of proteases. Therefore, the development of drugs targeting IL-8 expression is of great interest, since traditional drugs such as corticosteroids or ibuprofen have limited effect in CF. Importantly, in a study evaluating the effect of anti-

inflammatory drugs on the CF pulmonary pathophysiology, the nonsteroidal anti-inflammatory drug ibuprofen was reported to partially block CFTR-mediated chloride transport at pharmacologically relevant concentrations, thus potentially worsening the basic lung ion transport defect in CF (18). On the contrary, here we report that TMA, in addition to its anti-inflammatory effect, is able to potentiate CFTR dependent chloride efflux, suggesting that it already shows a dual-action that could be beneficially employed in CF in conjunction with other therapeutic strategies designed to increase mutated CFTR expression on apical membrane of bronchial cells and, in this way, help to both correct the ion transport defect and mitigate the excessive inflammation.

As far as the potential side effects of TMA are concerned, we should underline that TMA belongs to a class of furocoumarins (including angelicin and related molecules) applied for their antiproliferative activity in the therapeutic treatment of various skin diseases, because of their photosensitivity to UV light (23, 37). In this respect, it is known that the planar structure of furocoumarins helps them to intercalate between nucleic acid base pairs. Interestingly, in the case of linear furocoumarins, the psoralen monoadducts formed in the DNA can further react photochemically with a pyrimidine base on the complementary strand of the DNA, thus leading to interstrand cross-links (ICL). On the other hand, and relevant to biomedical applications, angular psoralens, such as TMA, allow only monofunctional DNA-binding upon irradiation with UV light, thus reducing undesirable side effects, especially long term ones, such as genotoxicity and risk of skin cancer (6, 7, 13, 23, 30). It is well known indeed that psoralens cause cell damage by covalent binding to DNA following UVA irradiation and these molecules exhibit a planar tricyclic structure with two photoreactive sites (3,4-pyrone and 4',5'-

furan double bonds). The initial intercalation and interaction with double stranded DNA is not characterized by covalent bonds but, upon absorption of a photon of UVA by furocoumarins moiety, a cycloaddition with the 5,6-double bond of pyrimidine residue (preferentially a thymine) of the DNA takes place. The resulting monoadduct can form a diadduct by absorbing a second photon, if a new pyrimidine on the opposite strand of DNA is available for an interstrand cross-link. On the contrary, angelicin and its angular analogues, are monofunctional isopsoralen isomers and cannot create interstrand cross-links because of the angular geometric structure (26, 31, 34). On the other hand, several recently published papers demonstrate biological activities of furocoumarins in the absence of UVA irradiation (1, 14). However, interactions with other molecules cannot be excluded and should be further explored. In any case, the activity of TMA here reported is not dependent from UVA irradiation and data available so far predict that drug concentrations suitable for IL-8 inhibition can be reached with no side effects, although thorough investigation on efficacy and safety in animal models will be required to support the concept that TMA can be proposed for anti-inflammatory treatment. Therefore, the inhibition of IL-8 expression by TMA encourages studies on *in vivo* experimental mouse models, since it predicts that TMA might inhibit *in vivo* IL-8 dependent recruitment of neutrophils in the bronchial lumen.

Preliminary results on the mechanism(s) by which TMA reduces IL-8 gene expression have been obtained by analyzing the effect of TMA on phosphoprotein kinases and on the interaction of NF- $\kappa$ B with IL-8 gene promoter. Here we confirm that *P.aeruginosa* activates MAP kinases ERK, JNK and p38 in bronchial epithelial cells, together with previously uncharacterized kinases, such as RSK1/2, MSK2, HSP27, GSK-3 and AKT1/2/3. Interestingly, TMA further

increases the phosphorylation of the MAP kinases, which are expected to play a proinflammatory role, the only reduction being observed for RSK1 and AKT 2/3. Although their pharmacological inhibition with triciribine hydrate and SL 0101-1 seems to confirm that RSK1 and AKT 2/3 are indeed relevant in the signaling pathway activating IL-8 gene transcription, further investigation is necessary to consolidate RSK1 and AKT 2/3 as molecular targets of TMA. Many laboratories including ours, proposed NF- $\kappa$ B as a key transcription factor activating IL-8 gene transcription. Here we found by EMSA experiments that TMA is able to bind NF- $\kappa$ B (Figure 11A) and reduces the *in vitro* interaction of NF- $\kappa$ B with oligonucleotides designed on its consensus sequence identified in the promoter of IL-8 gene only at mM concentration (Figure 11, B-D), which is many orders of magnitude higher than the nM concentrations inhibiting IL-8 gene transcription in whole cell experiments. Despite the fact that discrepancies between *in vitro* activities and effects on whole cellular systems are expected (22,35), these results suggest that TMA could intervene on other molecular targets leading to the sharp inhibition of IL-8 gene expression observed at nanomolar concentration. Interestingly, and in relation to this specific issue, chromatin immunoprecipitation assays allows to propose a very intriguing observation: (a) *Pseudomonas aeruginosa* infection leads to a sharp recruitment of NF- $\kappa$ B to the IL-8 gene promoter, supporting the role of NF- $\kappa$ B in the IL-8 gene transcription and IL-8 mRNA accumulation, and (b) TMA treatment strongly inhibits the NF- $\kappa$ B recruitment. Despite the fact that these data do not allow us to identify univocally the level(s) of TMA activity of the very complex NF- $\kappa$ B pathway, they support the hypothesis that, at least in part, IL-8 gene transcription is involved through interference on the positioning of NF- $\kappa$ B on the NF- $\kappa$ B binding sites present in

the IL-8 gene promoter. Further experiments using primers amplifying other gene promoters carrying NF- $\kappa$ B binding sites will clarify whether this effect is restricted to a specific class of NF- $\kappa$ B dependent genes.

Among additional cross-talks affected by TMA treatment, the effects on CFTR functions should be considered. Recently published observations, indeed, suggest a mechanism that links CFTR channel function to intracellular NF- $\kappa$ B signaling and inflammatory response (38). These studies support the concept that small molecules or therapeutic compounds that rescue optimal biological functions of mutant can attenuate the NF- $\kappa$ B mediated chronic inflammation. Our results could be considered in general agreement with the report by Vij and Coll (38), as we found that TMA potentiates CFTR function and in parallel inhibits NF- $\kappa$ B activity and IL-8 transcription. However, a new thorough investigation need to be pursued to confirm this potential mechanism of action.

The mechanism by which TMA potentiates CFTR function is completely unknown. Besides the original papers on the effect of psoralens on CFTR function (17), a larger panel of coumarin compounds from Chinese medicinal herbs have been recently published, both confirming the effect of angelicin or isopsoralen and identifying imperatorin and osthole as the two most effective potentiating compounds, with  $K_d$ s around 10  $\mu$ M (40). In principle, TMA, as reported here, seems more effective than imperatorin and osthole. Molecular modeling and docking studies of TMA into CFTR as protein target could help explaining the action mechanism of this potentiator and thus contribute to even better drug design for potentiating CFTR function.

In conclusion, in our opinion TMA deserves great attention and warrants further analyses to determine the mechanism of action on the modulation of the

immune response, on the molecular mechanism of potentiation of CFTR function and on the efficacy and safety in pre-clinical studies, in order to confirm its usefulness as an innovative therapeutic approach in CF lung disease.

### **Acknowledgments**

We are grateful to Maria Cristina Dececchi (Laboratory of Molecular Pathology, University-Hospital of Verona, Italy) and Stephan J. Reshkin (Dept of Physiology, University of Bari) for helpful discussions and suggestions, Alice Prince (Columbia University, NY, U.S.A.) for donating the *P. aeruginosa* laboratory strain PAO1 and to Federica Quiri for excellent technical assistance.



## REFERENCES

1. **Aboul-Enein HY, Kladna A, Kruk I, Lichszeld K, Michalska T.** Effect of psoralens on Fenton-like reaction generating reactive oxygen species. *Biopolymers*. 72: 59-68, 2003.
2. **Becker MN, Sauer MS, Muhlebach MS, Hirsh AJ, Wu Q, Verghese MW, Randell SH.** Cytokine secretion by cystic fibrosis airway epithelial cells. *Am. J. Respir. Crit. Care Med.* 169:645-653, 2004.
3. **Bezzerri V, Borgatti M, Nicolis E, Lampronti I, Dehecchi MC, Mancini I, Rizzotti P, Gambari R, Cabrini G.** Transcription factor oligodeoxynucleotides to NF-kappaB inhibit transcription of IL-8 in bronchial cells. *Am J Respir Cell Mol Biol.* 39:86-96, 2008.
4. **Black HR, Yankaskas JR, Johnson LG, Noah TL.** Interleukin-8 production by cystic fibrosis nasal epithelial cells after tumor necrosis factor-alpha and respiratory syncytial virus stimulation. *Am. J. Respir. Cell. Mol. Biol.* 19:210-2151, 1998.
5. **Bonfield TL, Panuska JR, Konstan MW, Hilliard KA, Hilliard JB, Ghnaim H, Berger M.** Inflammatory cytokines in cystic fibrosis lungs. *Am J Respir Crit Care Med* 152:2111-2118, 1995.
6. **Bordin F, Dall'Acqua F, Guiotto A.** Angelicins, angular analogs of psoralens: chemistry, photochemical, photobiological and phototherapeutic properties. *Pharmacol Ther* 52:331-363, 1991.
7. **Bordin F, Marzano C, Baccichetti F, Carllassare F, Vedaldi D, Falcomer S, Lora S, Rodighiero P.** Photobiological properties of 1'-thieno-4,6,4'-trimethylangelicin. *Photochem Photobiol* 68:157-163, 1998.
8. **Borgatti M, Bezzerri V, Mancini I, Nicolis E, Dehecchi MC, Lampronti**

- I, Rizzotti P, Cabrini G, Gambari R.** Induction of IL-6 gene expression in a CF bronchial epithelial cell line by *Pseudomonas aeruginosa* is dependent on transcription factors belonging to the Sp1 superfamily. *Biochem Biophys Res Commun.* 357: 977-83, 2007.
9. **Borgatti M, Lampronti I, Romanelli A, Pedone C, Saviano M, Bianchi N, Mischianti C, Gambari R.** Transcription factor decoy molecules based on a peptide nucleic acid (PNA)-DNA chimera mimicking Sp1 binding sites. *J. Biol. Chem.*, 278: 7500-7509, 2003.
10. **Borgatti M, Breda L, Cortesi R, Nastruzzi C, Romanelli A, Saviano M, Bianchi N, Mischianti C, Pedone C, Gambari R.** Cationic liposomes as delivery systems for double-stranded PNA-DNA chimeras exhibiting decoy activity against NF-kappaB transcription factors. *Biochem. Pharmacol.* 64: 609-616, 2002.
11. **Carpagnano GE, Barnes PJ, Geddes DM, Hodson ME, Kharitonov SA.** Increased leukotriene B4 and interleukin-6 in exhaled breath condensate in cystic fibrosis. *Am. J. Respir. Crit. Care Med.* 167:1109-1112, 2003.
12. **Chilin A, Marzano C, Guiotto A, Manzini P, Baccichetti F, Carllassare F, Bordin F.** Synthesis and biological activity of (hydroxymethyl)- and (diethylaminomethyl)-benzopsoralens. *J Med Chem* 42:2936–2945, 1999.
13. **Conconi MT, Montesi F, Parnigotto PP.** Antiproliferative activity and phototoxicity of some methyl derivatives of 5-methoxypsoralen and 5-methoxyangelicin. *Pharmacol Toxicol* 82:193–198, 1998.
14. **Dalla Via L, González-Gómez JC, Pérez-Montoto LG, Santana L, Uriarte E, Marciani Magno S, Gia O.** A new psoralen derivative with enlarged antiproliferative properties. *Bioorg Med Chem Lett.*

May 15;19(10): 2874-6, 2009 (Epub 2009 Mar 24).

15. **Dehecchi MC, Nicolis E, Bezzerri V, Vella A, Colombatti M, Assael BM, et al.** MPB-07 reduces the inflammatory response to *Pseudomonas aeruginosa* in cystic fibrosis bronchial cells. *Am J Respir Cell Mol Biol* 36:615-624, 2007.

16. **Dehecchi MC, Nicolis E, Norez C, Bezzerri V, Borgatti M, Mancini I, Rizzotti P, Ribeiro CM, Gambari R, Becq F, Cabrini G.** Anti-inflammatory effect of miglustat in bronchial epithelial cells. *J Cyst Fibros*. 7:555-65, 2008.

17. **Devor D.C., Singh A.K., Bridges R. J., and Frizzell R.A.** Psoralens: novel modulators of Cl<sup>-</sup> secretion. *American Journal of Physiology* 272: C976-988, 1997.

18. **Devor DC and Schultz BD.** Ibuprofen inhibits Cystic Fibrosis Transmembrane Conductance Regulator-mediated Cl<sup>-</sup> secretion. *J.Clin. Invest.* 102: 679-687, 1998.

19. **DiMango E, Zar HJ, Bryan R, Prince A.** Diverse *Pseudomonas aeruginosa* gene products stimulate respiratory epithelial cells to produce interleukin-8. *J Clin Invest* 96: 2204-2210, 1995.

20. **Favia M, Guerra L, Fanelli T, Cardone RA, Monterisi S, Di Sole F, Castellani S, Chen M, Seidler U, Reshkin SJ, Conese M, Casavola V.** Na<sup>+</sup>/H<sup>+</sup> exchanger regulatory factor 1 overexpression-dependent increase of cytoskeleton organization is fundamental in the rescue of F508del cystic fibrosis transmembrane conductance regulator in human airway CFBE410-cells. *Mol Biol Cell*. 21:73-86, 2010.

21. **Finotti A, Treves S, Zorzato F, Gambari R, Feriotto G.** Upstream stimulatory factors are involved in the P1 promoter directed transcription of

- the A beta H-J-J locus. *BMC Mol Biol.* 9:110, 2008.
22. **Gambari R, Borgatti M, Bezzerri V, Nicolis E, Lampronti I, Dehecchi M.C, Mancini I, Tamanini A, Cabrini G.** Decoy oligodeoxyribonucleotides and peptide nucleic acids-DNA chimeras targeting nuclear factor kappa-B: Inhibition of IL-8 gene expression in cystic fibrosis cells infected with *Pseudomonas aeruginosa*. *Biochem. Pharmacol.* 80: 1887-94, 2010.
23. **Guiotto A, Rodighiero P, Manzini P, et al.** 6-Methylangelicins: a new series of potential photochemotherapeutic agents for the treatment of psoriasis. *J Med Chem* 27:959–967, 1984.
24. **Jones AM, Martin L, Bright-Thomas RJ, Dodd ME, McDowell A, Moffitt KL, Elborn JS, Webb AK.** Inflammatory markers in cystic fibrosis patients with transmissible *Pseudomonas aeruginosa*. *Eur. Respir. J.* 22:503-506, 2003.
25. **Koehler DR, Downey GP, Swezey NB, Tanswell AK, Hu J.** Lung inflammation as a therapeutic target in cystic fibrosis. *Am J Respir Cell Mol Biol* 31:377-381, 2004.
26. **Komura J, Ikehata H, Hosoi Y, Riggs AD, Ono T.** Mapping psoralen cross-links at the nucleotide level in mammalian cells: suppression of cross-linking at transcription factor- or nucleosome-binding sites. *Biochemistry* 40:4096–4105, 2001.
27. **Kube DM, Fletcher D, Davis PB.** Relation of exaggerated cytokine responses of CF airway epithelial cells to PAO1 adherence. *Respir. Res.* 6:69, 2005.
28. **Ma T, Tiagarajah JR, Yang H, Sonawane ND, Folli C, Galletta LJ, Verkman AS** Thiazolidinone CFTR inhibitor identified by high-throughput

screening blocks cholera toxin-induced intestinal fluid secretion. *J. Clin. Invest.* 110:1651-1658, 2002.

29. **Maestro** (v7.0.113) – A unified interface for all Schrodinger products, developed and marketed by Schrodinger, LLC. NY, Copy-right 2005, <http://www.schrodinger.com>.

30. **Marzano C, Caffieri S, Fossa P, Bordin F.** Activity of 3-carbetoxyangelicin photolysis products. *J Photochem Photobiol B* 38:189–195, 1997.

31. **Mosti L, Lo Presti E, Menozzi G, Marzano C, Baccichetti F, Falcone G, Filippelli W, Piucci B.** Synthesis of angelicin heteroanalogues: preliminary photobiological and pharmacological studies. *Farmaco* 53:602–610, 1998.

32. **Nicolis E, Lampronti I, Dehecchi MC, Borgatti M, Tamanini A, Bianchi N, Bezzerri V, Mancini I, Giri MG, Rizzotti P, Gambari R, Cabrini G.** Pyrogallol, an active compound from the medicinal plant *Emblica officinalis*, regulates expression of pro-inflammatory genes in bronchial epithelial cells. *Int Immunopharmacol.* 8:1672-80, 2008.

33. **Nicolis E, Lampronti I, Dehecchi MC, Borgatti M, Tamanini A, Bezzerri V, Bianchi N, Mazzon M, Mancini I, Giri MG, Rizzotti P, Gambari R, Cabrini G.** Modulation of expression of IL-8 gene in bronchial epithelial cells by 5-methoxypsoralen. *Int Immunopharmacol.* 9:1411-22, 2009.

34. **Parrish JA.** Phototherapy and photochemotherapy of skin diseases. *J Invest Dermatol* 77:167–171, 1981.

35. **Piccagli L, Borgatti M, Nicolis E, Bianchi N, Mancini I, Lampronti I, Vevaldi D, Dall'acqua F, Cabrini G, Gambari R.** Virtual screening against

nuclear factor  $\kappa$ B (NF- $\kappa$ B) of a focus library: Identification of bioactive furocoumarin derivatives inhibiting NF- $\kappa$ B dependent biological functions involved in cystic fibrosis. *Bioorg Med Chem.* in the press, 2010.

36. **Puchelle E, De Bentzmann S, Hubeau C, Jacquot J, Gaillard D.** Mechanisms involved in cystic fibrosis airway inflammation. *Pediatr Pulmonol* S23:143-145, 2001.

37. **Stern RS.** Psoralen and ultraviolet A light therapy for psoriasis. *N Engl J Med* 357:682-690, 2007.

38. **Vij N, Mazur S, Zeitlin PL.** CFTR is a negative regulator of NF $\kappa$ B mediated innate immune response. *PLoS One.* 4:e4664, 2009.

39. **Welsh MJ, Tsui L-C, Boat TF, Beaudet AL.** Cystic fibrosis. In: *The metabolic and molecular bases of inherited disease.* Edited by Scriver CR, Beaudet AL, Sly WS, Valle D, New York, McGraw-Hill Inc, 3799-3876, 1995.

40. **Xu LN, Na WL, Liu X, Hou SG, Lin S, Yang H, Ma TH.**

Identification of natural coumarin compounds that rescue defective DeltaF508-CFTR chloride channel gating. *Clin. Experimen. Pharmacol. Physiol.* 35: 878-883, 2008.

41. **Zabner J, Karp P., Seiler M., Phillips S.L., Mitchell C.J., Saavedra M., Welsh M., Klingelutz A.J.** Development of cystic fibrosis and noncystic fibrosis airway cell lines. *Am. J. Physiol. Lung Cell Mol. Physiol.* 284:L844-L854, 2003.

## Figure legends

**Figure 1.** Chemical structures of the linear and angular psoralens utilized in this study.

**Figure 2.** Effect of PSR (A), TMP (B), ANG (C) and TMA (D) on *P.aeruginosa*-dependent IL-8 transcription in IB3-1 cells. The cells were infected for 4 h with PAO1 strain (20 CFU/cell) after 24 h incubation with the indicated concentrations of different compounds. IL-8 mRNA was quantified by qRT-PCR and reported as % of IL-8 mRNA copies expressed in PAO1-infected cells. Data are mean  $\pm$  S.E.M. of at least 3 independent experiments performed in duplicate, the error bars at 0.001 and 0.01  $\mu$ M are inside of the size of filled circles.

**Figure 3.** Effects of PSR and TMP on pro-inflammatory genes expression in Calu-3 monolayers. The non-CF bronchial epithelial cells Calu-3 have been grown up to confluence on Transwell<sup>®</sup> insert filters and exposed to PAO1 on the apical side in the presence of 10  $\mu$ M PSR (A) or TMP (B). Results have been expressed as mRNA fold induction over the basal transcript level. Data are mean  $\pm$  SEM of at least 3 independent experiments performed in duplicate.

**Figure 4.** Effects of ANG on pro-inflammatory genes expression in Calu-3 (A) and CuFi-1 (B) monolayers. The non-CF bronchial epithelial cells, Calu-3 and the CF bronchial epithelial cells, CuFi-1 have been grown up to confluence on Transwell<sup>®</sup> insert filters and exposed to PAO1 on the apical side in the presence of 10  $\mu$ M ANG.

**Figure 5.** Dose-response effect of TMA in CuFi-1 cells. A, B: Cells were grown on 2-cm-diameter wells ( $2.5 \times 10^5$  cells/well). After adhesion, fresh medium was replaced and the cells were treated with the indicated concentrations of TMA, 20 hrs before bacterial exposure. A: IL-8 mRNA accumulation and B: IL-8 protein release are reported. C: Similar to panels A and B, here TMA (100 nM) was added 20 hours before infection or simultaneously with *P.aeruginosa*.

**Figure 6.** Effects of TMA on pro-inflammatory genes expression in Calu-3 (A) and CuFi-1 (B) monolayers. The non-CF bronchial epithelial cells, Calu-3 and the CF bronchial epithelial cells, CuFi-1 have been grown up to confluence on Transwell<sup>®</sup> insert filters and exposed to PAO1 on the apical side in the presence of 100 nM TMA as reported in Material and Methods.

**Figure 7.** Effect of TMA on *P.aeruginosa*-dependent IL-8 transcription in CFBE41o- and CFBE41o-/NHERF1. The cells have been grown up to confluence on Transwell<sup>®</sup> insert filters and exposed to PAO1 on the apical side in the presence of 100 nM TMA as reported in Material and Methods.

**Figure 8.** Functional analysis of CFTR dependent chloride efflux in Calu-3 cell monolayers. A and C, typical recordings showing changes in intracellular Cl<sup>-</sup>-dependent MQAE fluorescence (expressed as the  $F/F_0$  ratio) cell monolayers, grown on permeable filters, in the absence or presence of 250 nM TMA. TMA has been added (to both sides of the monolayer) 15 min. before nitrate substitution and remained for the entire chloride efflux (Figure 8, panel C). Figure 8, panels B



and D, shows the summary of the data collected from different experiments respectively in Calu-3 in absence (panel B,  $n=4$ ) or in presence of TMA (panel D,  $n=5$ ). CFTR dependent chloride efflux (*empty bar*) was calculated as the difference in the  $F/F_0$  ratio ( $\Delta(F/F_0)/\text{min}$ ) in the absence (dark bar) and presence of (light gray bar) of  $5\mu\text{M}$  CFTRinh-172. Statistical analysis has been made by paired Student's t test with respect to the chloride efflux stimulated by FSK measured in the absence of CFTR<sub>inh</sub>-172.

**Figure 9.** Effect of TMA on CFTR-dependent chloride efflux. A: Concentration-response of CFTR-dependent chloride efflux to TMA in Calu-3 cell monolayers, expressing wt CFTR. The CFTR dependent chloride efflux was determined as described in Figure 8. B: Effect of TMA (250 nM) on CFTR dependent chloride efflux measured in CFBE41o- expressing F508del CFTR and in CFBE41o- /sNHERF1 overexpressing NHERF1 in which F508del CFTR has been rescued on the apical membrane. Each bar represents the mean  $\pm$  S.E. Statistical comparison has been made using unpaired Student's t-test with respect to control CFTR-dependent chloride efflux.

**Figure 10.** Phosphorylation pattern of kinases in CuFi-1 cells treated with TMA and infected with *P. aeruginosa*. TMA (100 nM) was added 20 hours before exposure to bacteria or medium alone for an additional 30 minutes. Cell lysates were collected and analysed using the Human Phospho-MAPK Array Kit as described in Materials and Methods. A: The panel shows the signal of the spots of 21 phosphorylated kinases obtained after incubation of different cell lysates with nitrocellulose membranes. B: The intensity of the signal of each spot presented in

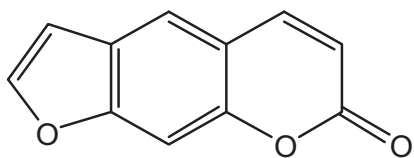
panel A has been quantified with Digimizer image analysis software and represented as bar graph. The numbers indicate the correspondent kinases in panels A and B. C: Effect of phosphokinase inhibitors on *P. aeruginosa* dependent IL-8 mRNA induction. CuFi-1 cells were incubated with the inhibitors of Akt 1,2,3 and RSK, Triciribine hydrate (1  $\mu$ M) and SL 0101-1 (2  $\mu$ M), respectively, for 1 hour before exposure to bacteria and throughout the 4 hrs infection period. Data are mean  $\pm$  SEM of 3 to 5 independent experiments performed in duplicate.

**Figure 11.** Effects of TMA on NF- $\kappa$ B/DNA interactions. Stereo view of the complex formed by NF- $\kappa$ B p50 homodimer and the docked TMA. The amino acids Tyr57, Cys59 and Lys 145, involved in the interactions with TMA, are highlighted. (B-D) Effects of TMA on the molecular interactions between NF- $\kappa$ B p50 (B), NF- $\kappa$ B p50/p65 (C) or nuclear extracts from IB3-1 cells (D) and  $^{32}$ P-labeled target NF- $\kappa$ B double stranded oligonucleotide. In the upper part of panel B TMA was first incubated with NF- $\kappa$ B and then  $^{32}$ P-labelled target NF- $\kappa$ B oligonucleotide was added. In the lower part of panel B and in panels C and D, TMA was first incubated with NF- $\kappa$ B and then the  $^{32}$ P-labelled target NF- $\kappa$ B oligonucleotide was added. NF- $\kappa$ B/DNA complexes were analyzed by polyacrylamide gel electrophoresis. Arrows indicate NF- $\kappa$ B/DNA complexes; asterisks indicate the  $^{32}$ P-labelled target NF- $\kappa$ B probe.

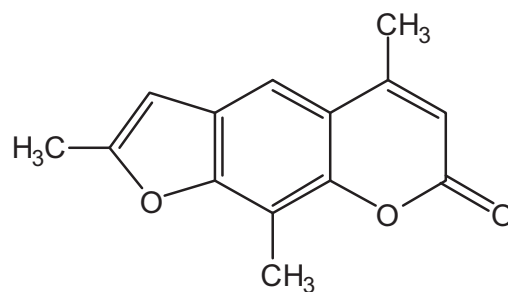
**Figure 12.** Interaction of NF- $\kappa$ B transcription factor with the IL-8 gene promoter. A: Schematic representation of IL-8 gene promoter region. The sequences homologous to transcription factors binding sites are boxed. The location of primers used for IL-8 promoter amplification in ChIP assay and the product length

are also indicated. B: PCR product containing NF-kB binding site, obtained from IL-8 promoter amplification (IL-8 prom) and PCR product obtained using control primers flanking a genomic region about 5 Kb upstream of IL-8 promoter (IL-8 neg). C: Quantitative real-time PCR profiles for the amplification of the IL-8 promoter are shown for a representative ChIP assay in which chromatin from IB-3 cells was immunoprecipitated using NF-kB p65 antiserum. The data (from duplicate determinations) demonstrate the early exponential increase in fluorescence as a result of SYBR Green I incorporation into the amplifying IL-8 promoter fragment. PAO, PAO+TMA indicate duplicate curves from chromatin that have been immunoprecipitated with NF-kB antiserum, respectively; (-) indicates curves from immunoprecipitations of untreated cells with NF-kB antiserum (cross marked lines). Input represents curves obtained from untreated IB3 cells chromatin (1%) before immunoprecipitation. The cycle at which the amplification curve reaches threshold fluorescence (TF), the threshold cycle, were used to determine the relative amounts of promoter in each sample. D: *In vivo* association of NF-kB transcription factor with the IL-8 promoter. The results, obtained from ChIP assay quantitative real-time PCR using negative control IgG and NF-kB antiserum, were analyzed following the methodology described in Experimental procedures. The fold increase compares the values obtained by IL-8 gene promoter amplification of untreated IB3 cells (-) with IB3 treated with *P.aeruginosa* or *P.aeruginosa* plus TMA.

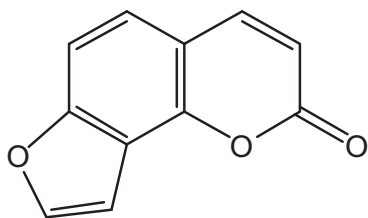
Figure 1



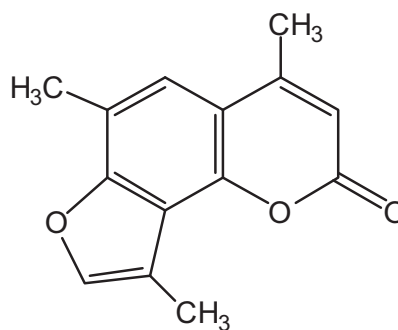
**Psoralen**  
(PSO)



**4,5',8-Trimethylpsoralen**  
(TMP)



**Angelicin**  
(ANG)



**4,6,4'-Trimethylangelicin**  
(TMA)

Figure 2 A,B,C and D

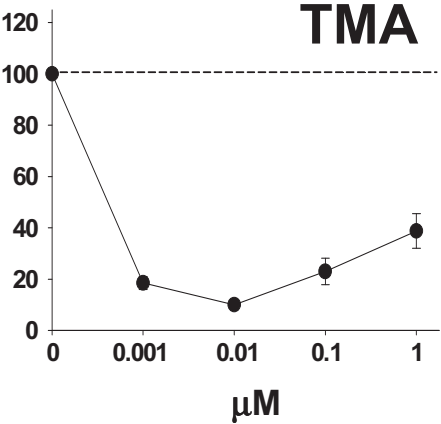
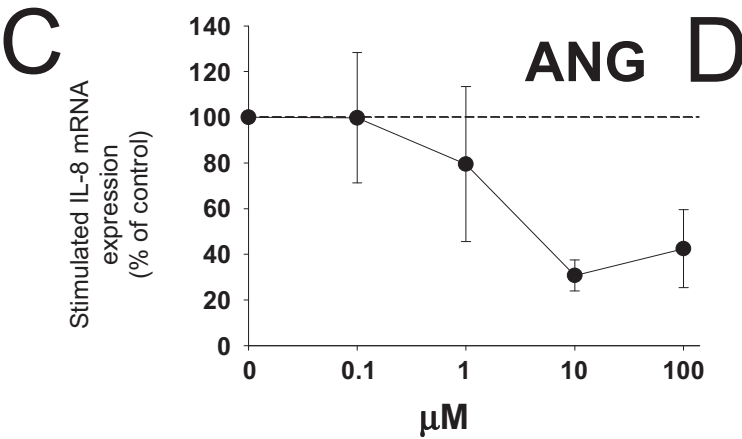
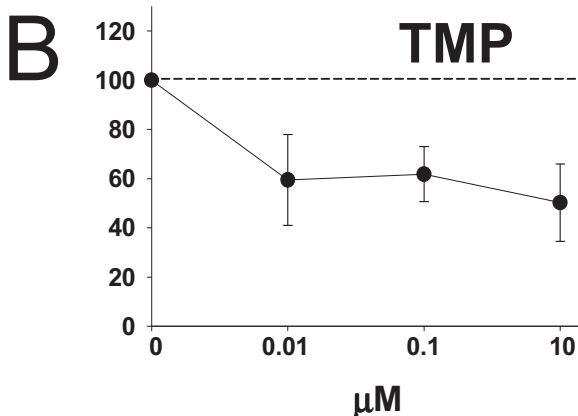
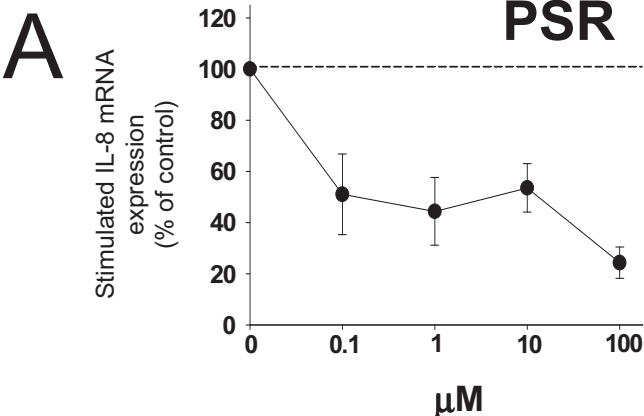


Figure 3 A and B

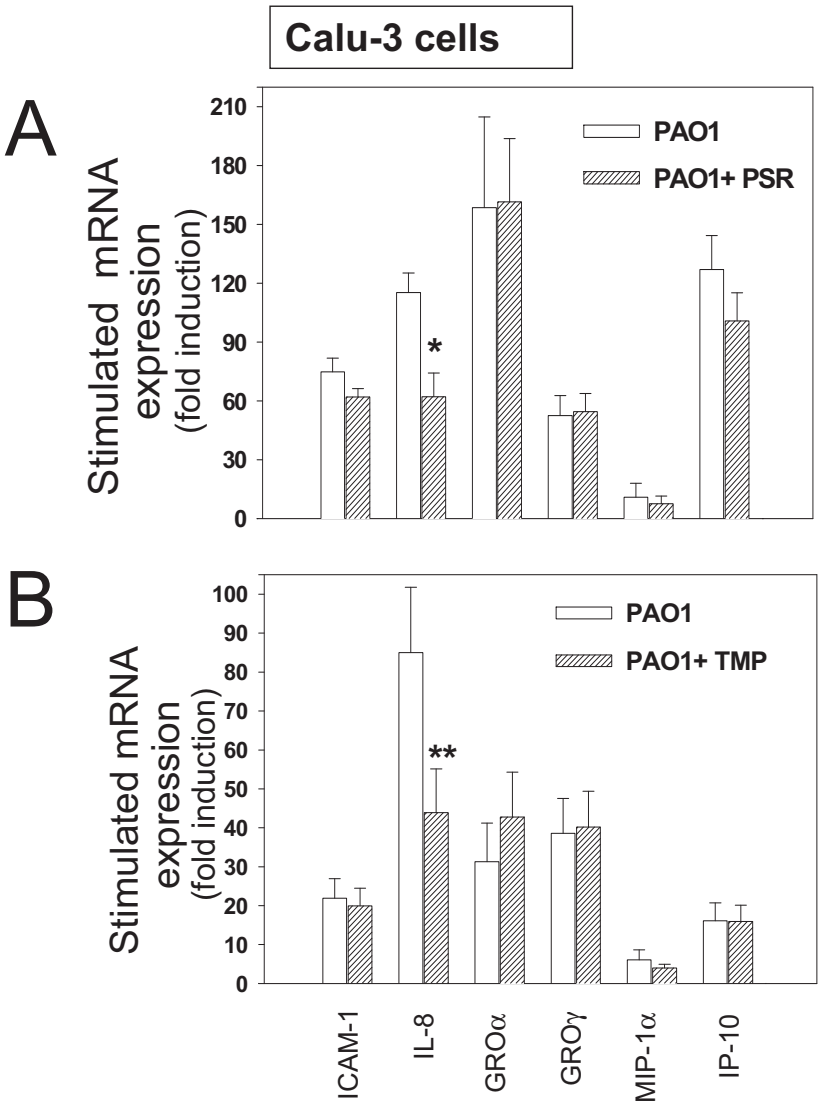


Figure 4 A and B

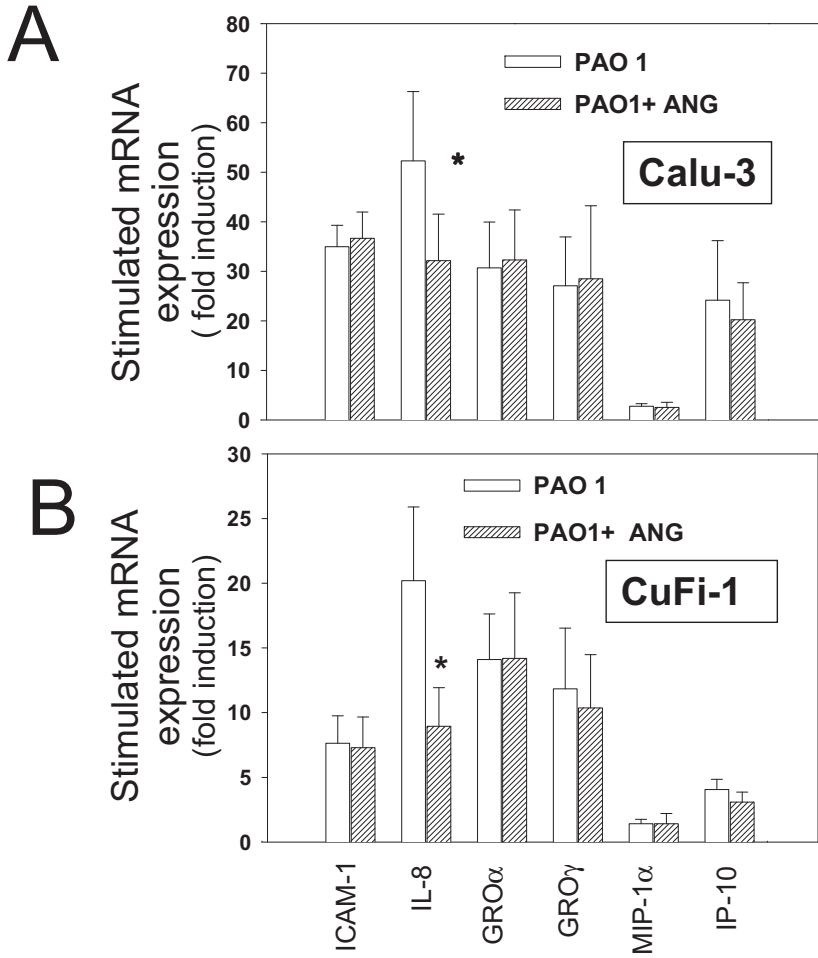


Figure 5 A, B and C

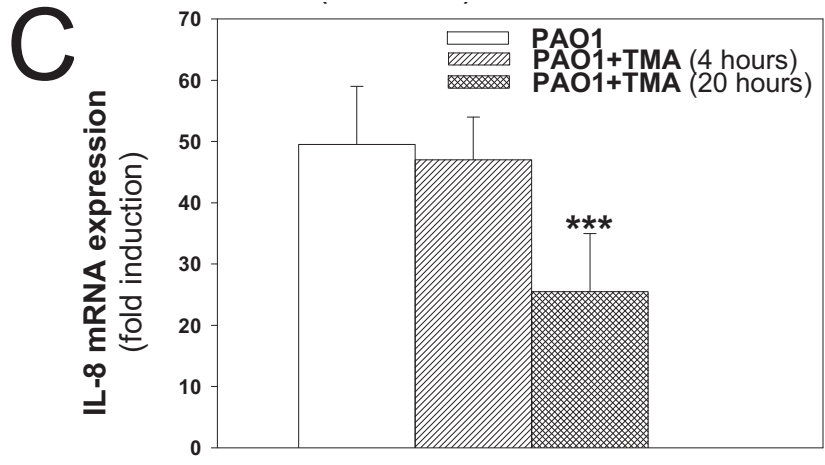
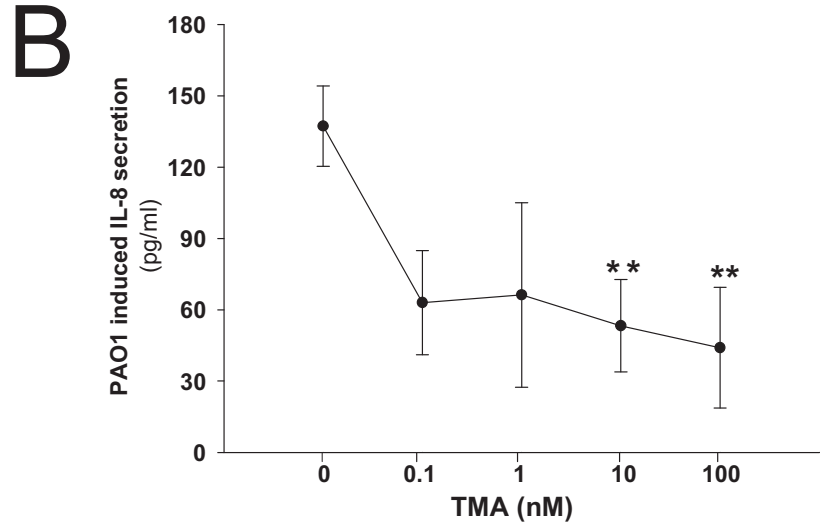
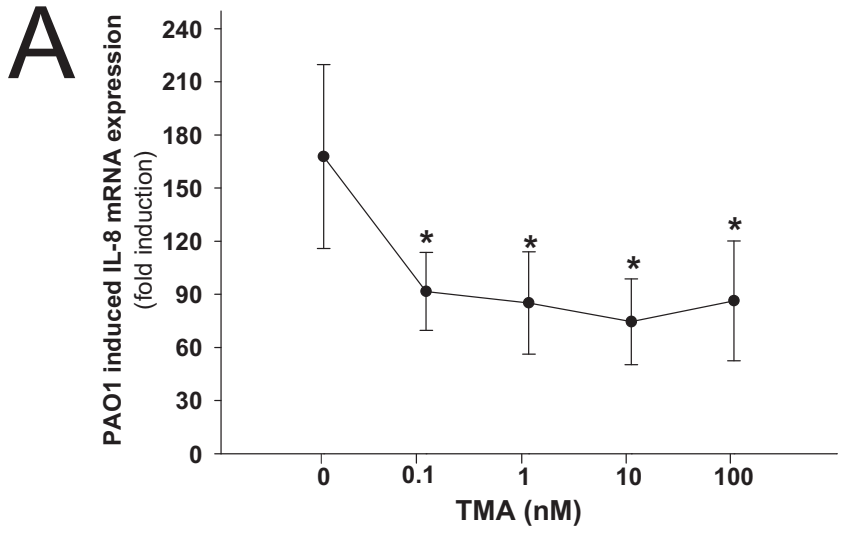
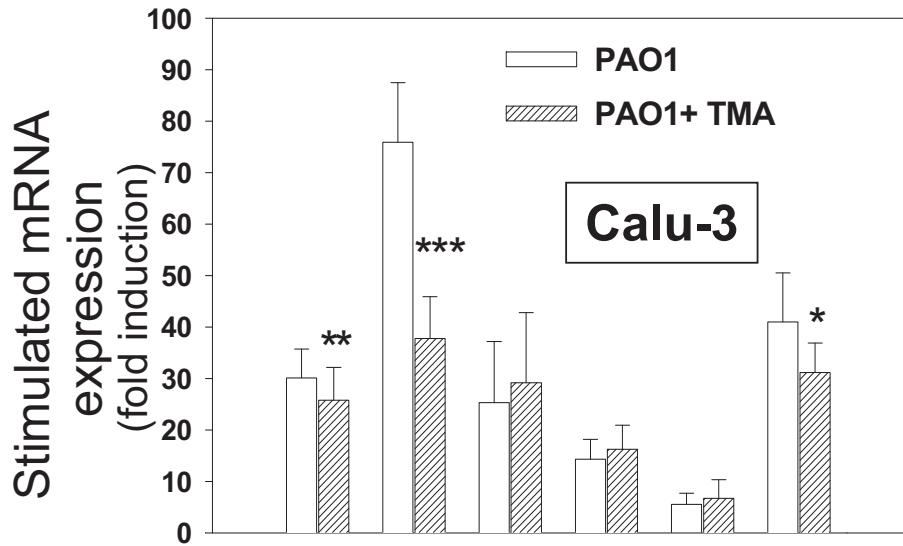




Figure 6 A and B

**A**



**B**

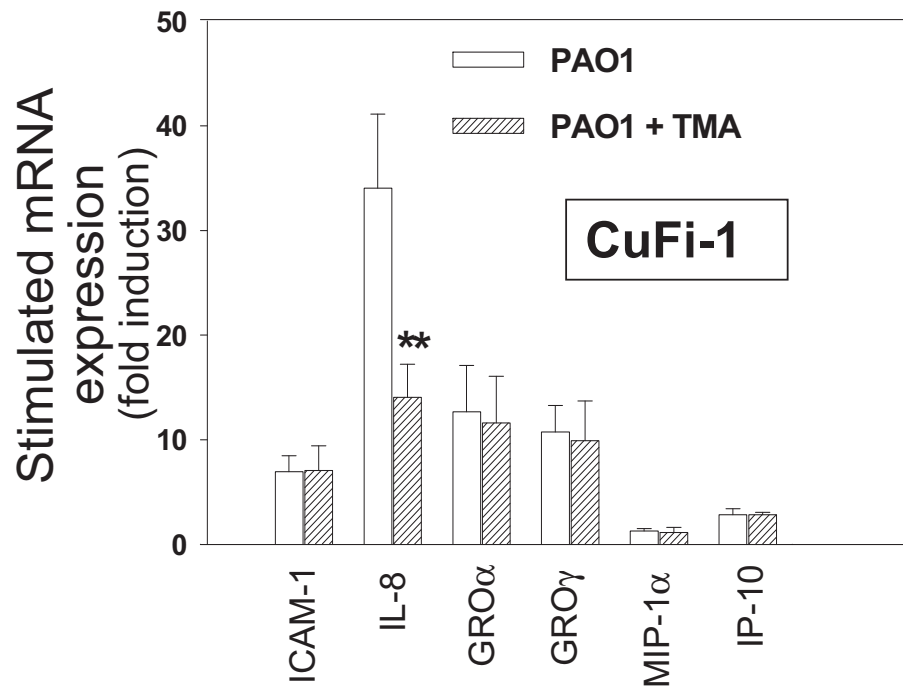


Figure 7

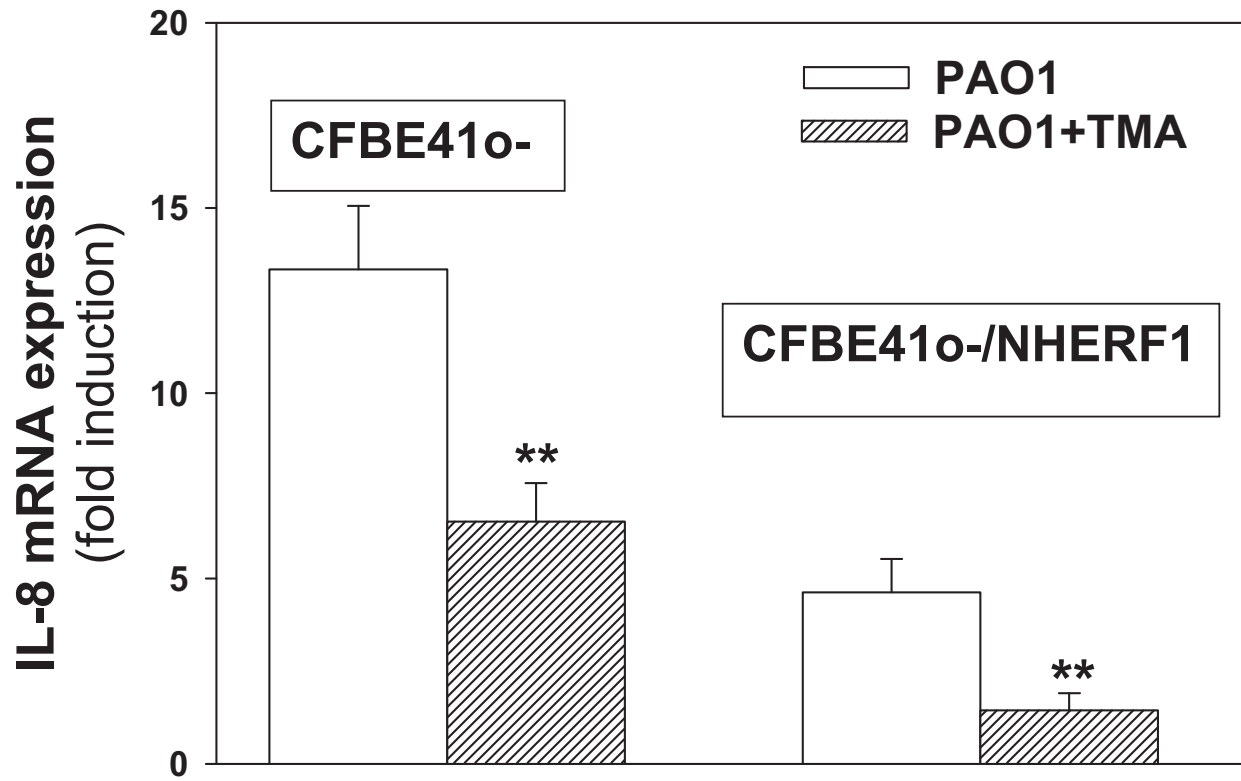


Figure 8 A, B, C and D

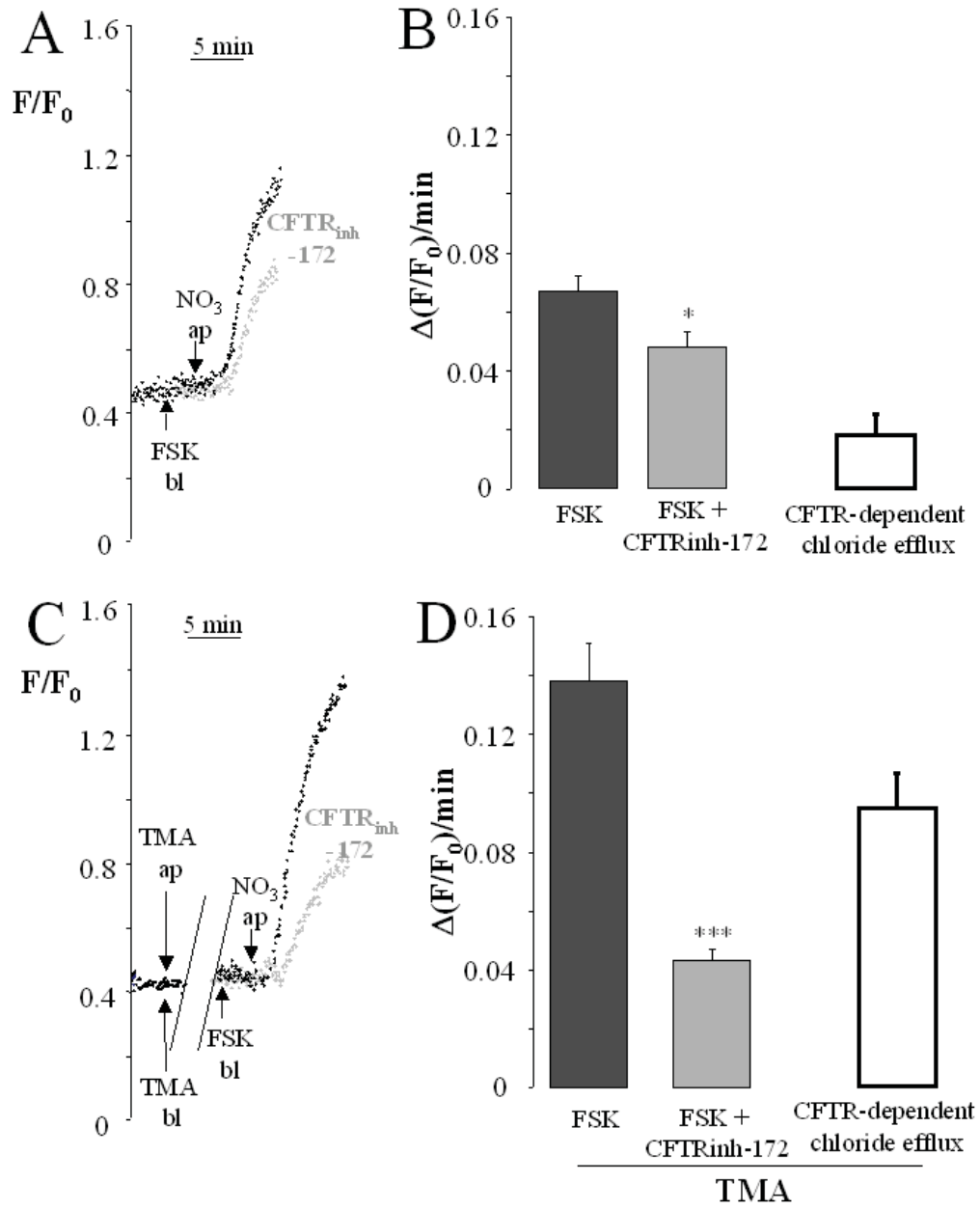


Figure 9 A and B

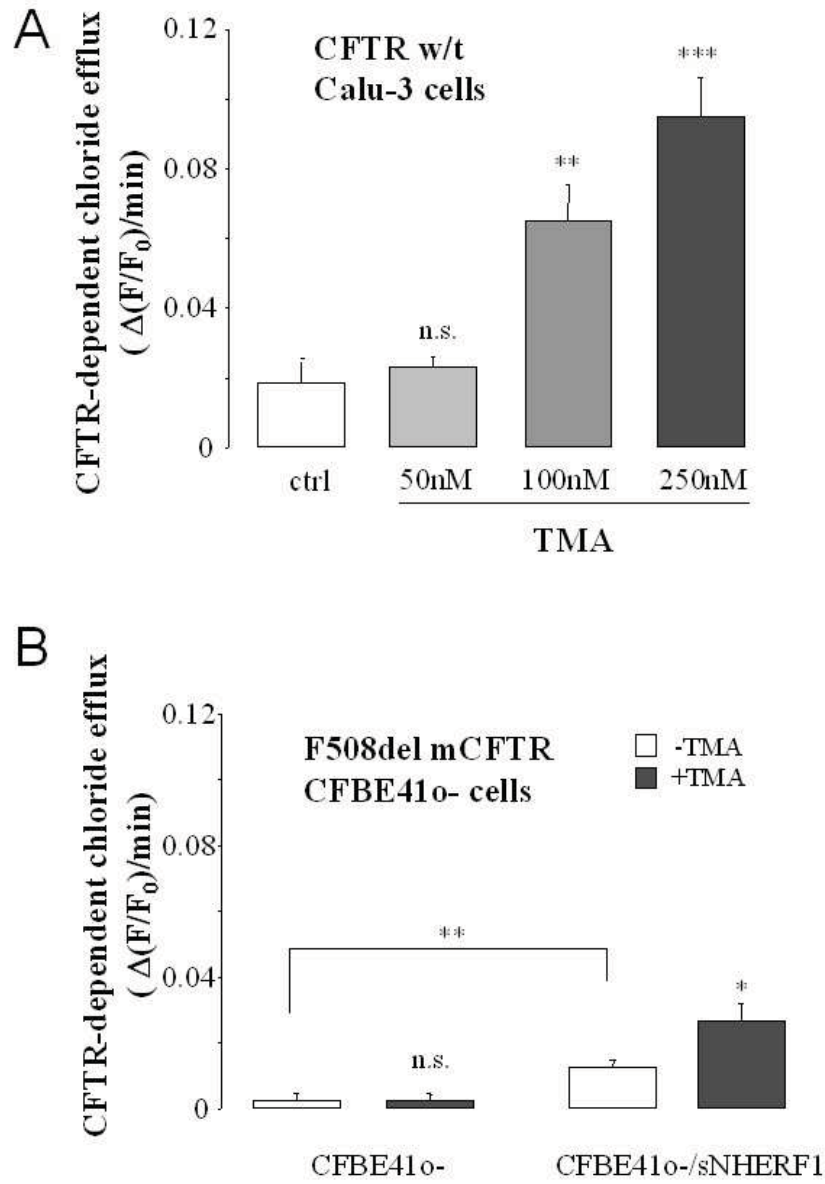


Figure 10 A, B and C

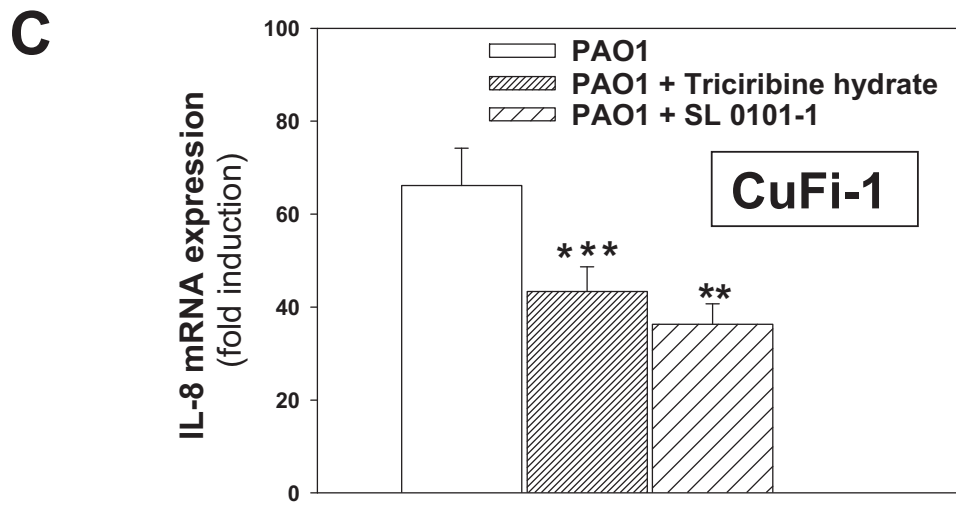
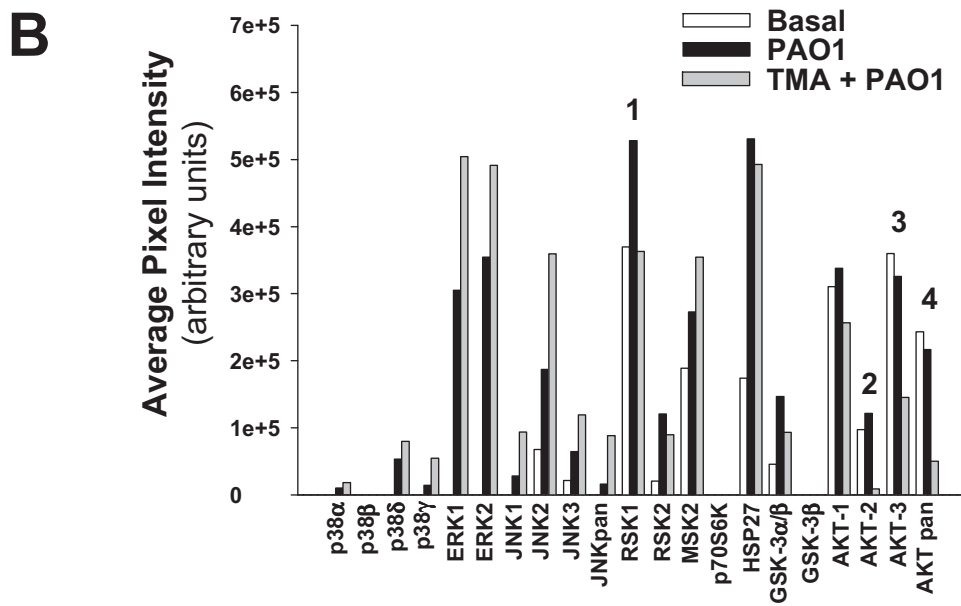
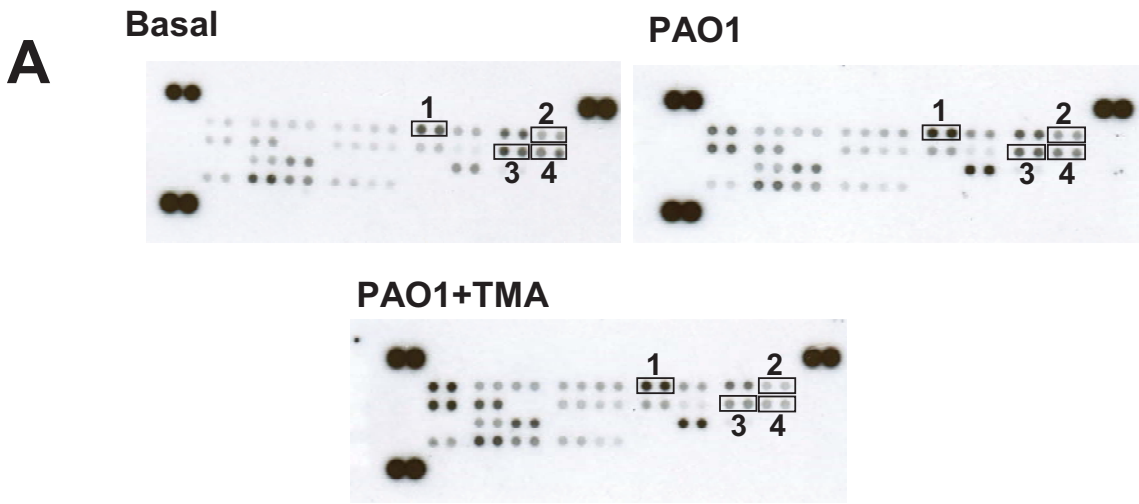


Figure 11 A, B, C and D

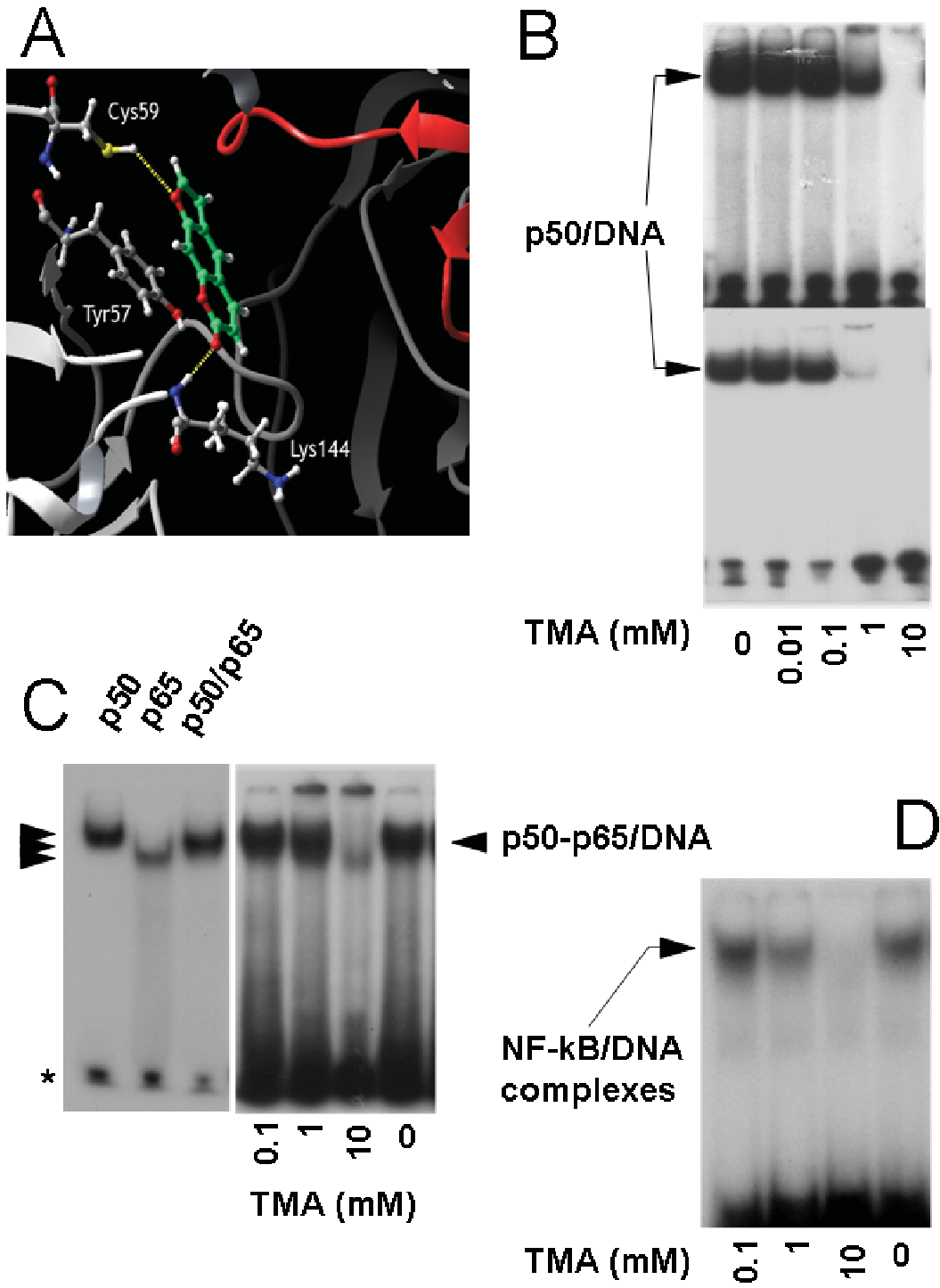


Figure 12 A, B, C and D

